A 1305
A New Model of PEMFCs: Process Identification from Physics-based EIS Simulation

Georg Futter[1], Arnulf Latz[1,2], Thomas Jahnke[1]

1: German Aerospace Center (DLR), Stuttgart, Germany

2: Helmholtz Institute Ulm for Electrochemical Energy Storage (HIU), Ulm, Germany

Motivation

Why physical modeling of fuel cells?

- Better understanding of processes in the cell and their interaction
- Insights on experimentally inaccessible properties
- Simulation based prediction of cell performance and lifetime
- Optimization of cell performance and durability

Challenges:

- Complex system: coupling of processes on very different time and length scales
- Details of the involved mechanisms often unknown and material dependent
- Heterogeneities within the cell require 2D and 3D cell models

Modeling Approach

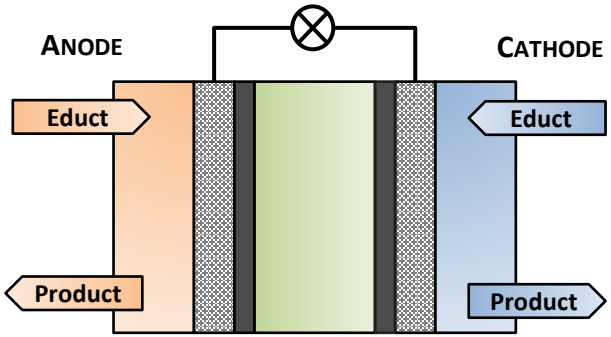

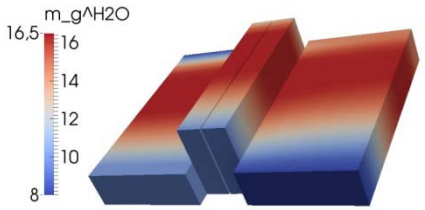

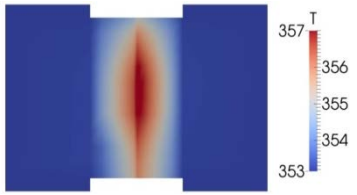

Multi-scale cell models

Model validation

Degradation models

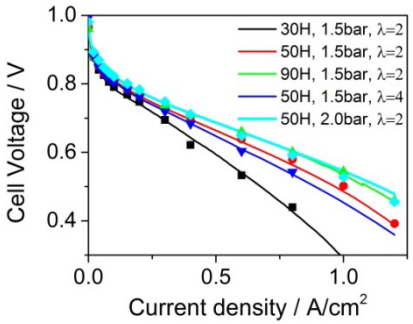

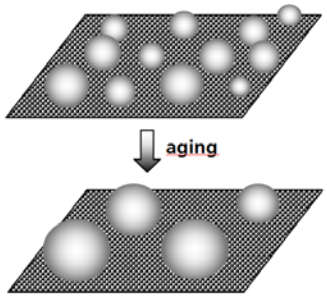

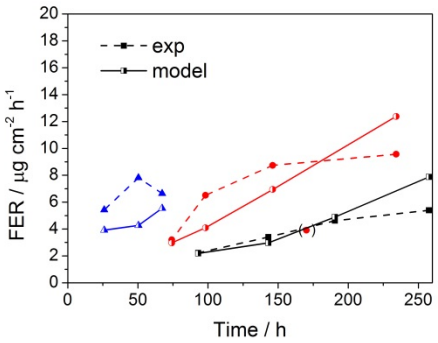

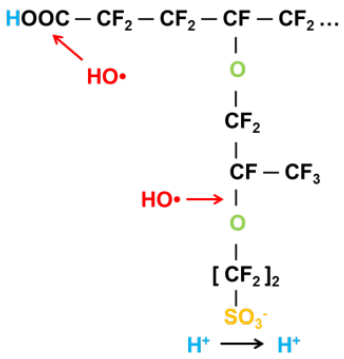

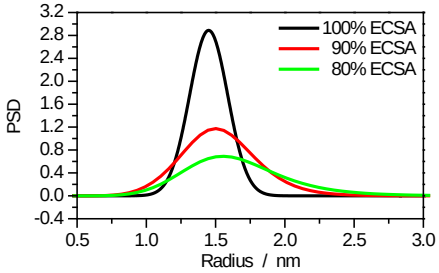

NEOPARD-FC/EL: Numerical Environment for the Optimization of Performance And Reduction of Degradation of Fuel Cells/ELectrolyzers

- Modeling framework to investigate fuel cell/electrolyzer performance and degradation
- Developed at DLR since 2013 based on the open source software DuMu^X [1]

NEOPARD-FC features

- 2D and 3D discretizations of the cells
- Transport models for the cell components
- Electrochemistry models
- Specific fluid systems for the different technologies
- Transient simulations (e.g. impedances)

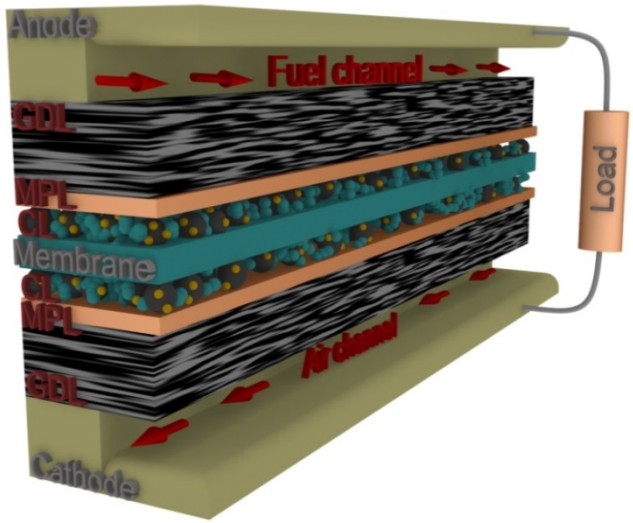

Field of Application:

- PEMFC
- DMFC
- SOEC

[1]: Flemisch et al., **2011**, *Adv. Water Resour.*, *34*(9).

PEMFC Model Features

- 9 layers spatially resolved (channels, GDLs, MPLs, CLs, PEM)
- Two-phase multi-component transport model
- Charge transport in ionomer phase
- Ionomer film model in the CLs
- ORR: BV kinetics with doubling of Tafel slope
- Platinum oxide model
- Gas crossover through membrane
- Non-isothermal
- Realistic boundary conditions: lambda-control at fixed back pressure in potentiostatic and galvanostatic mode

$$K_1 = \frac{\lambda_{H_3O^+}}{(1-\lambda_{H_3O^+})(\lambda_{H_2O}-\lambda_{H_3O^+})\exp(\Phi_1\lambda_{H_3O^+})\exp(\Phi_2\lambda_{H_2O})} \qquad a_{H_2O} = K_2(\lambda_{H_2O}-\lambda_{H_3O^+})\exp(\Phi_2\lambda_{H_3O^+})\exp(\Phi_3\lambda_{H_2O})$$

$$D^{\kappa}_{pm,g} = (S_g\phi)^{1.5}\left(\frac{1}{D^{\kappa}_{Knudsen}} + \frac{1}{\tilde{D}^{k}_{g}}\right)^{-1} \qquad D^{\kappa}_{Knudsen} = r\frac{2}{3}\sqrt{\frac{8RT}{\pi M^k}}$$

$$\xi^{\kappa} = \phi\sum_{\alpha=1}^{M}\rho_{mol,\alpha}x^{\kappa}_{\alpha}S_{\alpha} \qquad \Psi^{\kappa} = \sum_{\alpha=1}^{M}\left(\frac{k_{r,\alpha}}{\mu_{\alpha}}\rho_{mol,\alpha}x^{\kappa}_{\alpha}K\nabla p_{\alpha} + D^{\kappa}_{pm,\alpha}\rho_{mol,\alpha}\nabla x^{\kappa}_{\alpha}\right)$$

$$p_c = \frac{2\sigma\cos\theta}{r} \qquad \Psi = S\left(-\frac{\sigma n_{drag,l}}{F}\nabla\Phi - \left(\alpha_l + \frac{\sigma n^2_{drag,l}}{F^2}\right)\nabla\mu_{H_2O}\right)$$

$$+(1-S)\left(-\frac{\sigma n_{drag,v}}{F}\nabla\Phi - \left(\alpha_v + \frac{\sigma n^2_{drag,v}}{F^2}\right)\nabla\mu_{H_2O}\right)$$

$$\frac{\partial\xi^{\kappa}}{\partial t} + \nabla\cdot\Psi^{\kappa} - q^{\kappa} = 0$$

$$r = \frac{\sqrt{4A_{eff}n^2F^2c_{O2} + R^2k^2} - Rk}{2A_{eff}nF}k$$

$$k = ECSA\, i_o c^{-0.5}_{ref}\left[\exp\left(\frac{\alpha nF\eta}{RT}\right) - \exp\left(\frac{(1-\alpha)nF\eta}{RT}\right)\right]$$

$$-\frac{\partial C_{DL}(\Phi_{elde}-\Phi_{elyte})}{\partial t} + \nabla\cdot\left(-\sigma^{H^+}_{eff}\nabla\Phi_{elyte}\right) - q^{H^+} = 0 \qquad q^{PtOx} = k^{PtOx}\begin{bmatrix} a^{H_2O}\exp\left(\frac{-E_{act}}{RT}\theta^{PtOX}\right) \\ \times(1-\theta^{PtOX})\exp\left(\frac{\alpha^{PtOx}F\eta^{PtOx}}{RT}\right) \\ -\theta^{PtOX}\exp\left(-\frac{\alpha^{PtOx}F\eta^{PtOx}}{RT}\right)\end{bmatrix}$$

$$\eta^{i} = \Phi_{elde} - \Phi_{elyte} - E_0{}^{i}$$

Open Questions

I. What are the contributions to experimentally measured impedance spectra?

II. What are possible explanations for inductive phenomena observed at low frequencies[1]?

[1]: Pivac & Barbir , **2015**, *J. Power Sources*, *326, 112-119*.

Model Validation

- Model validation under various operating conditions is important for reliability
  - Different RH
  - Different pressure
  - Different stoichiometry

- Strong effect of RH on cell performance (Tafel slope + transport)
- High stoichiometry at 50% RH leads to lower performance
  → drying out overcompensates higher oxygen partial pressure

- Model validation successful?

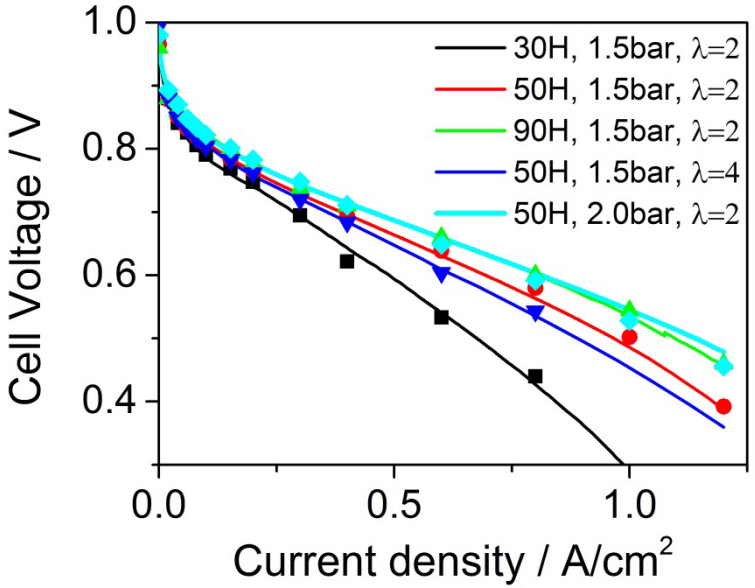

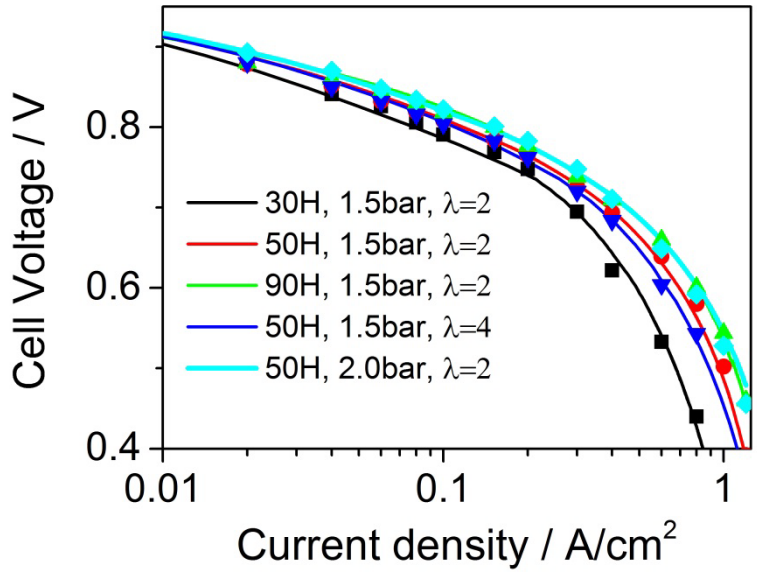

Model Validation

Impedance measurements at various current densities for 30% RH and 50% RH:

- Trends and frequencies are correctly described by the model
- Total values still show a significant deviation
- Inductive feature at low frequency can explain the difference between low frequency resistance and slope of iV-curve

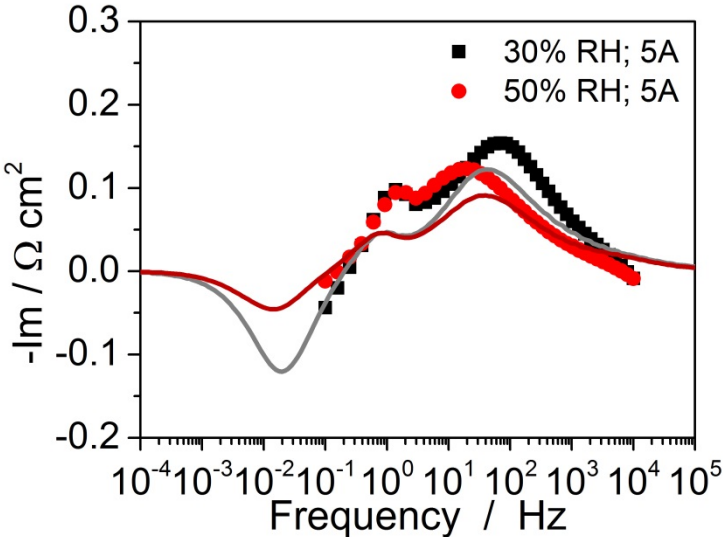

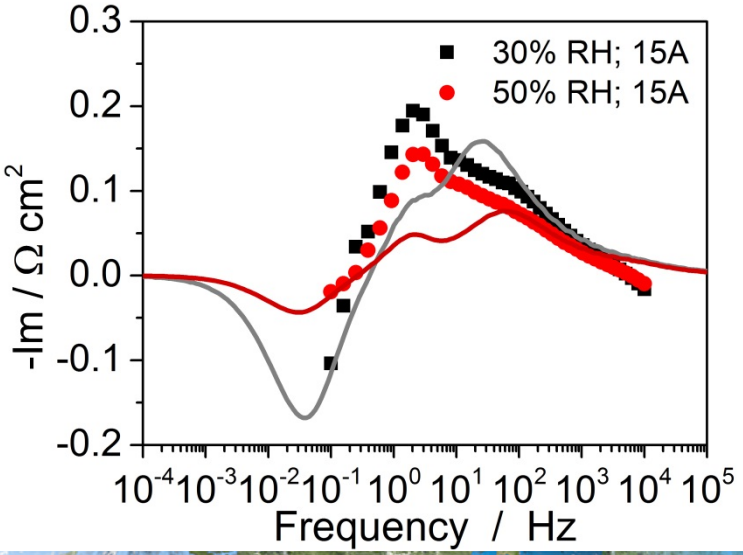

Process Identification from EIS Simulation

Ionomer

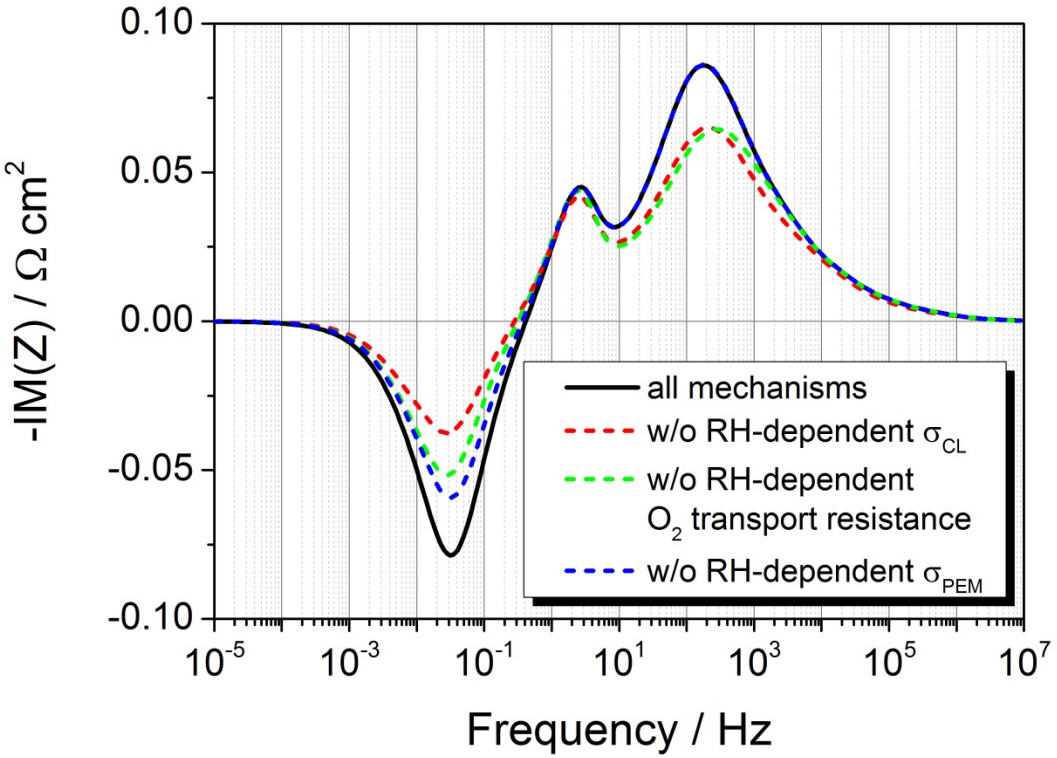

- Strong dependence of ionic conductivity on RH [1,2] causes inductive behavior (PEM and CCL)
- Same effect for O_2 transport resistance in the CCL ionomer

[1]: D. K. Paul et al., JES, 161 (**2014)** F1395.
[2]: B. P. Setzler, F. Fuller JES, 162 (**2015)** F519.

Process Identification from EIS Simulation

Electrochemistry

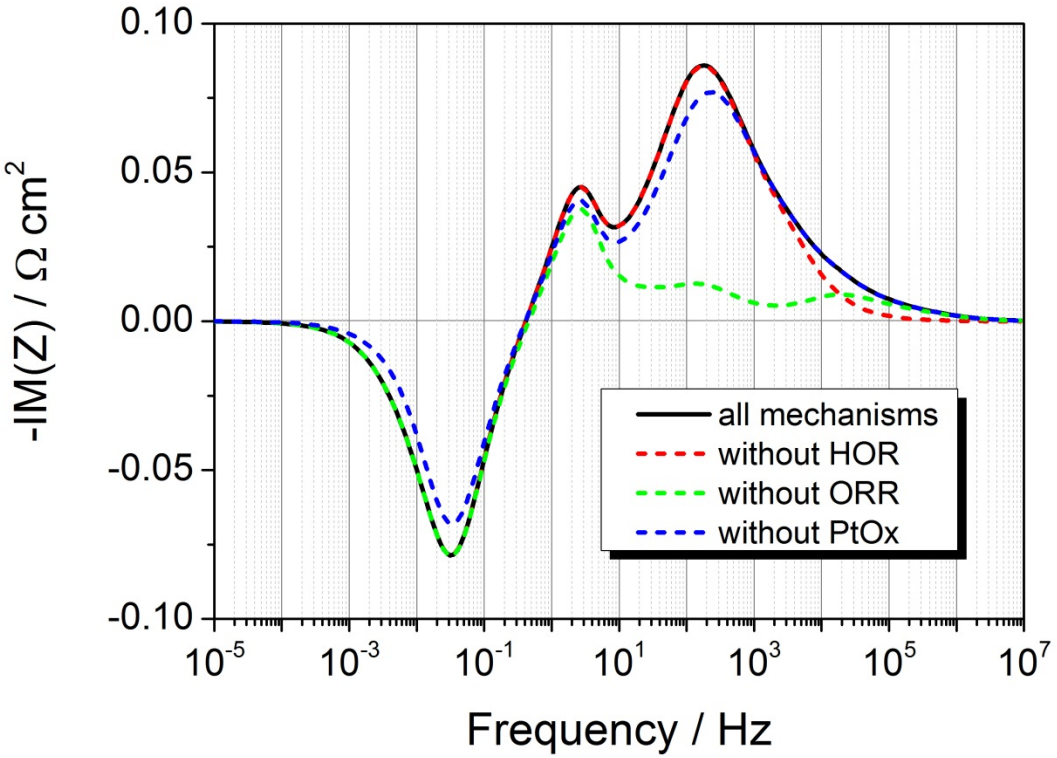

- HOR at ~10^4 Hz
- ORR at ~10^2 Hz:
  - HOR and Diffusion peaks are revealed
- PtOx-formation causes inductive behavior at ~10^{-2} Hz

Process Identification from EIS Simulation

Transport

Concentration gradients in the cell

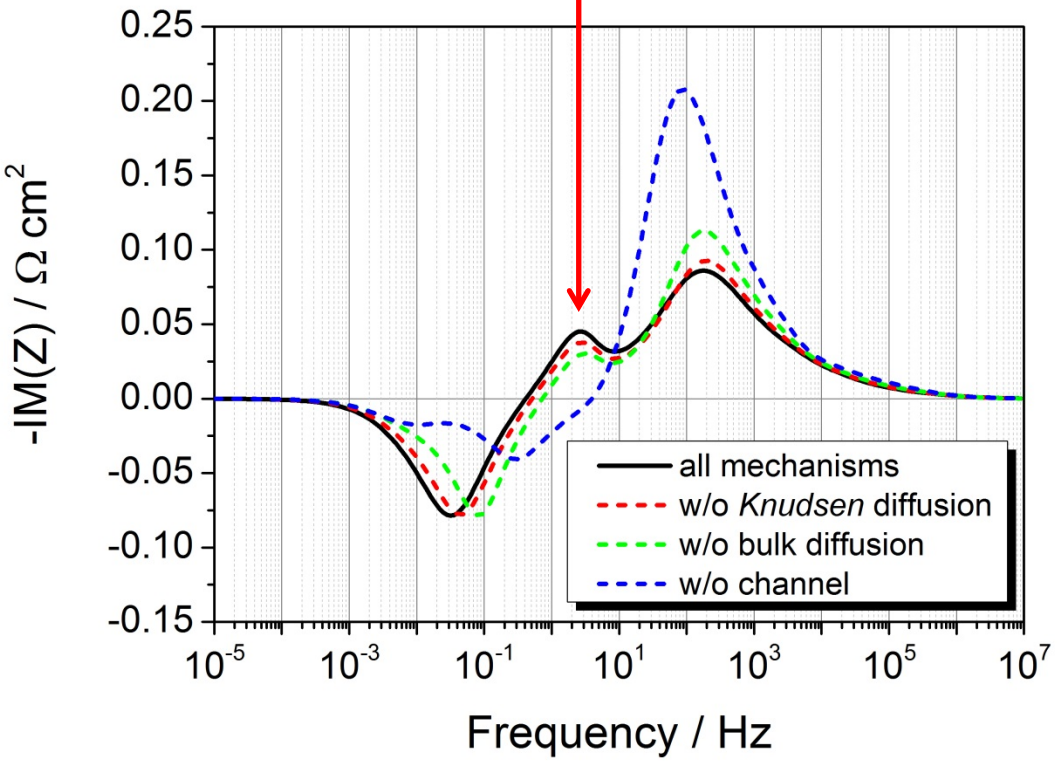

- Knudsen and bulk diffusion are operative at ~10^2 Hz
- Reduced hydration outweighs improved O_2 concentration → reduced cell performance
- Concentration gradients along the channel cause capacitive peak at ~1 Hz

Model validation revisited

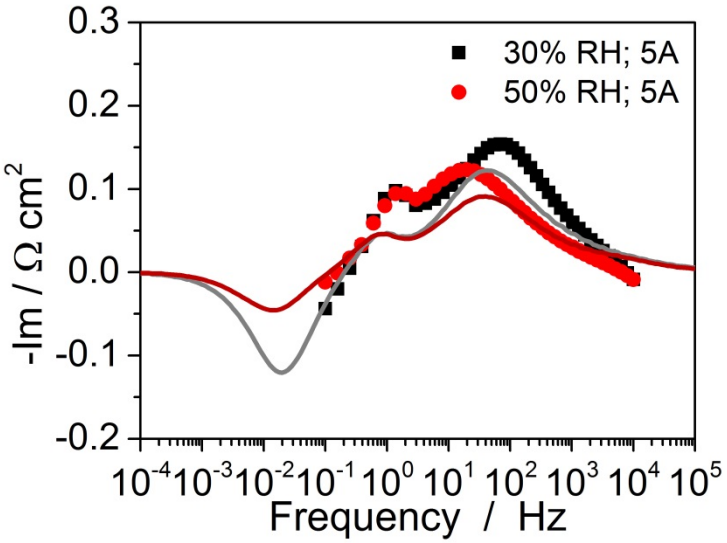

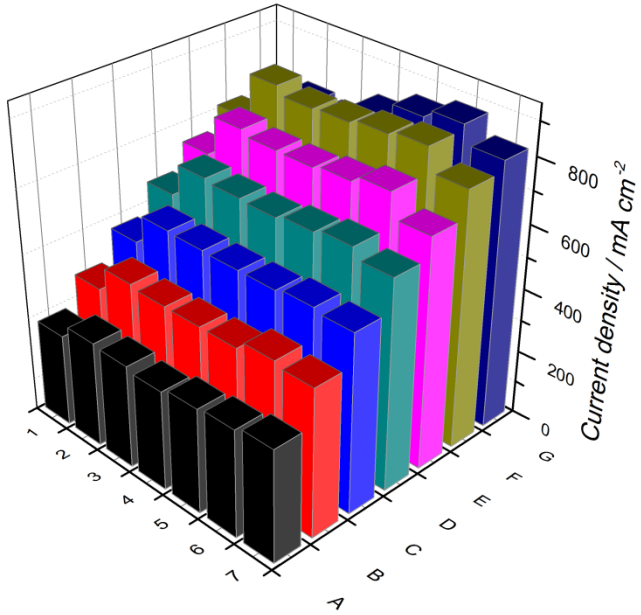

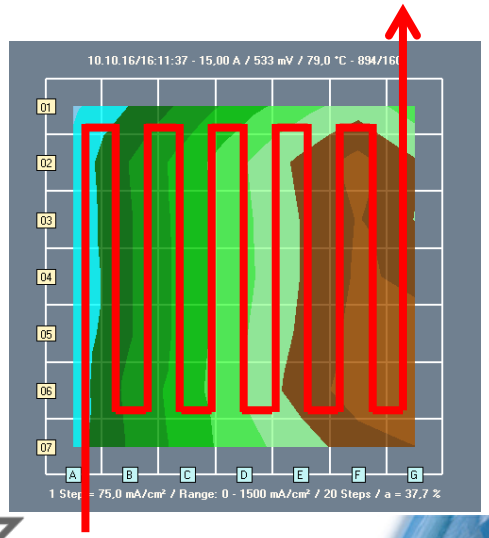

Schematic! In reality 24 bends along the flow channel

- Unknown effect at the cell borders leads to reduced cell performance
- Stronger concentration gradients inside the cell (3D effects?) can explain the deviation of model and experiment

Summary

- The development of predictive fuel cell models is challenging:
  - Complex interplay of many mechanisms on various time and length scales
  - Strong gradients within the cell require the development of 2D and 3D models
  - Model validation has to be performed under various operating conditions, ideally including the simulation of impedances to ensure model reliability

- Inductive phenomena, observed in EIS at low frequencies (~10^{-2} Hz) may be caused by:
  - Platinum oxide formation
  - RH-dependent ionic conductivity of the ionomer
  - Further RH-dependent mechanisms (O_2 transport resistance in the CCL)

"It can scarcely be denied that the supreme goal of all theory is to make the irreducible basic elements as simple and as few as possible without having to surrender the adequate representation of a single datum of experience“

Albert Einstein

Thank you for your attention

Process Identification from EIS Simulation

EIS without all mechanism

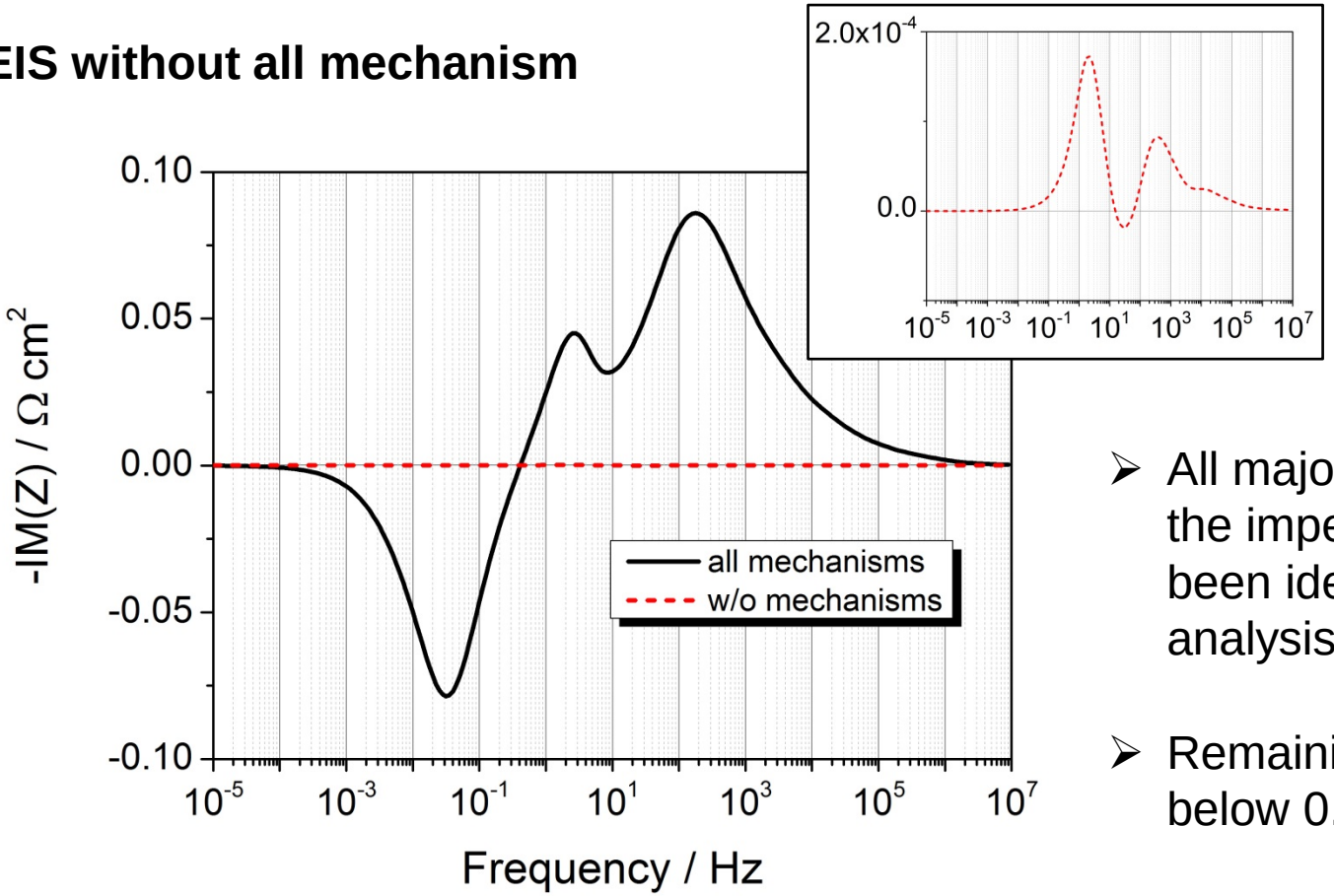

- All major contributions to the impedance have been identified in the analysis
- Remaining features are below 0.2 mΩ cm²

Process Identification from EIS Simulation

Cathode transport analysis

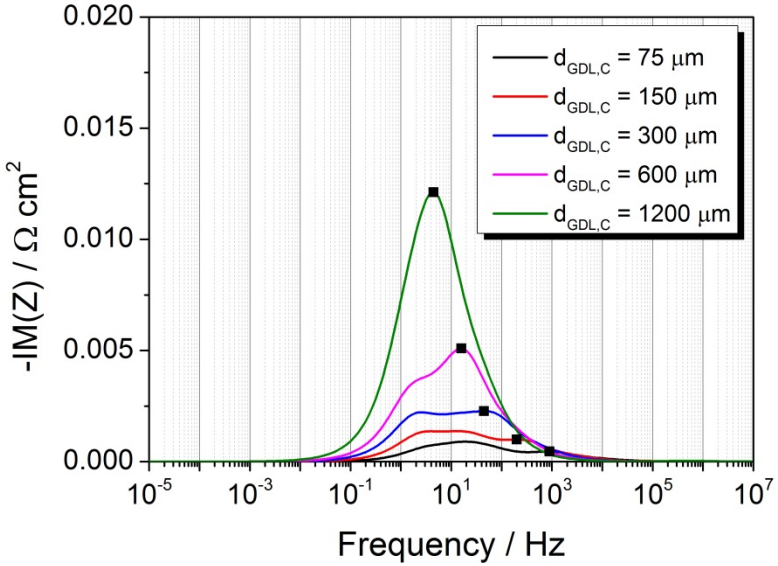

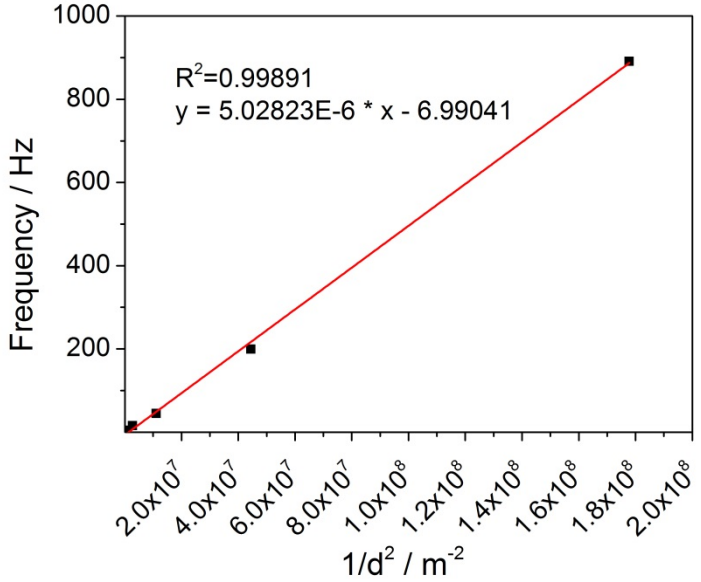

- Increasing GDL thickness results in higher diffusion resistance
  → negligible compared to concentration gradients due to geometry

- Frequency of the diffusion peak: $f \sim 1/d^2$
  → in accordance with Einstein-Smoluchowski relation: $f = \frac{2D}{d^2}$

Process Identification from EIS Simulation

Anode transport analysis

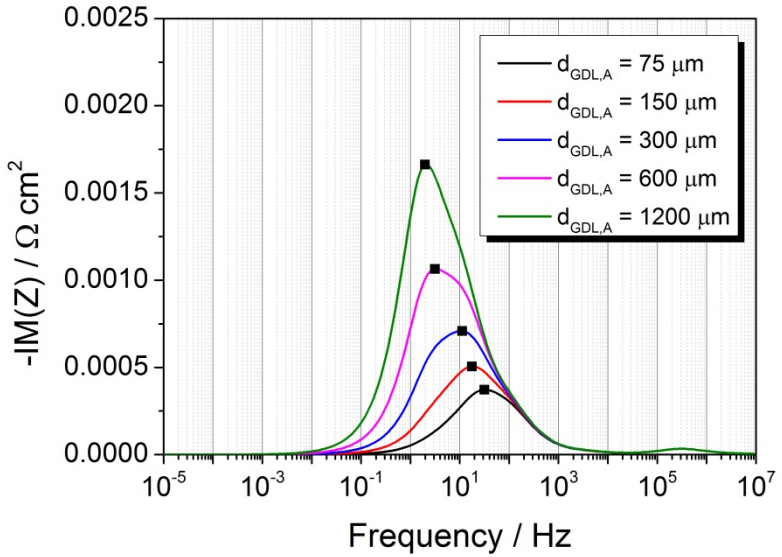

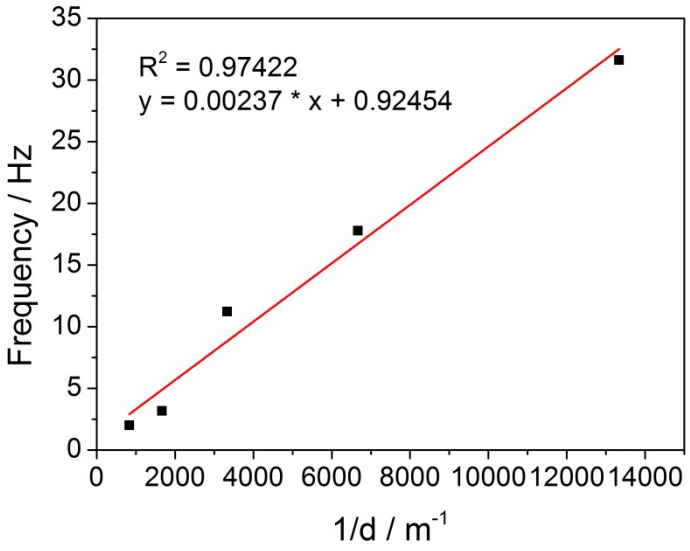

- Increasing GDL thickness results in higher resistance due to diffusion and **convection**
- Frequency of the convection peak: f ~ 1/d

Process Identification from EIS Simulation

Transport analysis

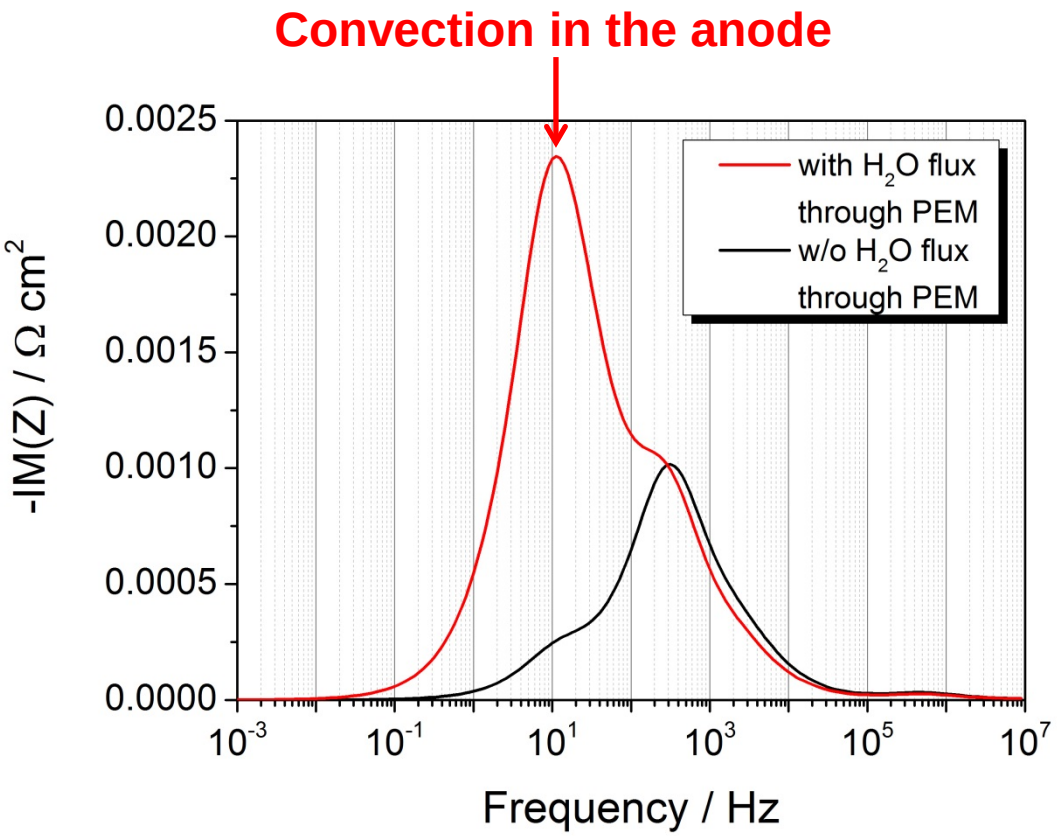

- Electroosmotic H_2O flux through the PEM causes convective transport in the anode

Cathode catalyst utilization

ORR reaction rate distribution

- Location of maximum reaction rate and distribution strongly depends on operating conditions
- At high RH
  - Very homogeneous at low current densities
- At low RH
  - Strong heterogeneities along channel
  - A significant part of the CCL is not used

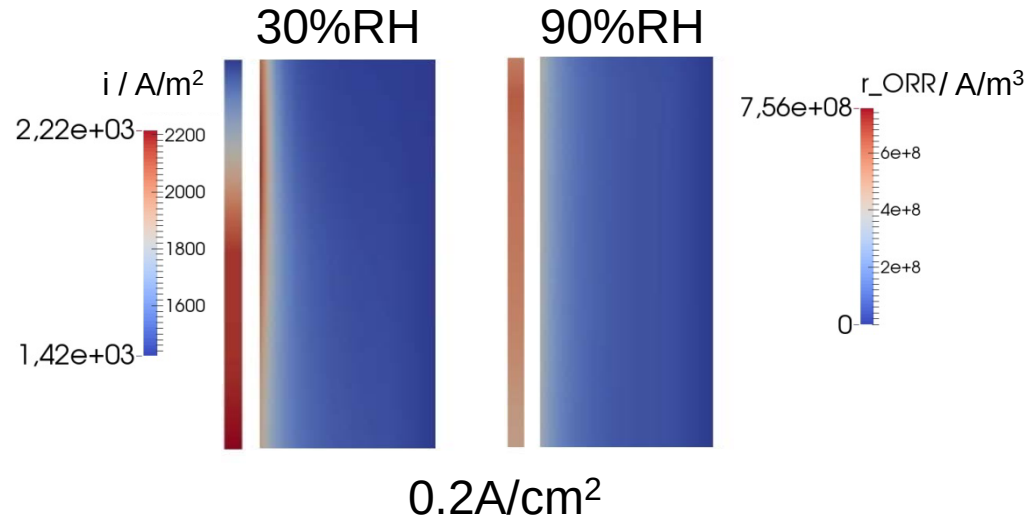

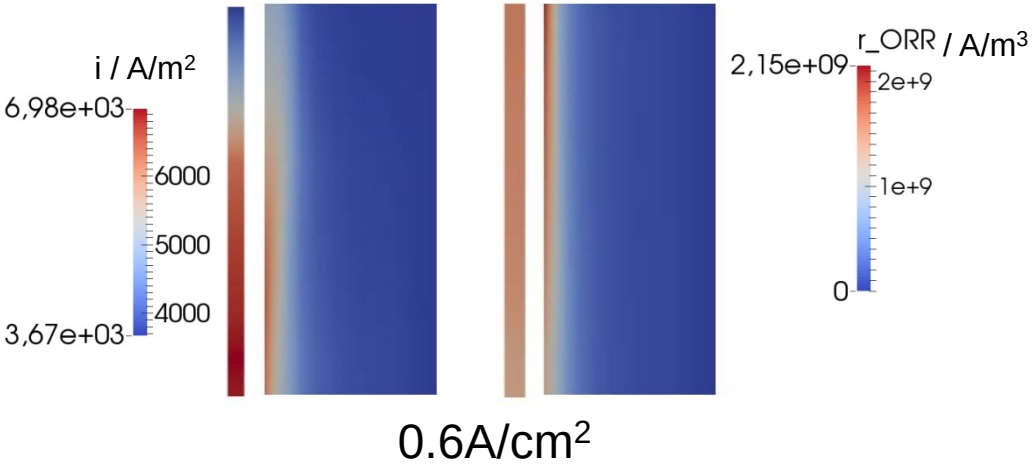

Two-phase transport model

- Multiphase Darcy approach + nonlinear complementarity function for robust treatment of phase transitions[1]
  - Arbitrary number of phases → here: gas + liquid
  - Arbitrary number of components

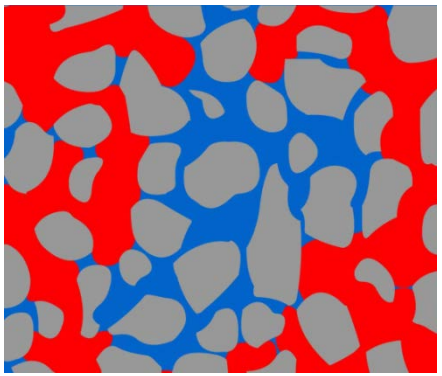

$$\frac{\partial \xi^{\kappa}}{\partial t} + \nabla \cdot \Psi^{\kappa} - q^{\kappa} = 0; \qquad \xi^{\kappa} = \phi \sum_{\alpha=1}^{M} \rho_{mol,\alpha} x_{\alpha}^{\kappa} S_{\alpha}$$

$$\Psi^{\kappa} = \sum_{\alpha=1}^{M} \left(\frac{k_{r,\alpha}}{\mu_{\alpha}} \rho_{mol,\alpha} x_{\alpha}^{\kappa} K \nabla p_{\alpha} + D_{pm,\alpha}^{\kappa} \rho_{mol,\alpha} \nabla x_{\alpha}^{\kappa} \right)$$

- Knudsen diffusion in gas phase

$$D_{pm,g}^{\kappa} = \left(S_g \phi\right)^{1.5} \left(\frac{1}{D_{Knudsen}^{\kappa}} + \frac{1}{\tilde{D}_g^{k}} \right)^{-1}; \qquad D_{Knudsen}^{\kappa} = r \frac{2}{3} \sqrt{\frac{8RT}{\pi M^{k}}}$$

[1]: Lauser et al., **2011**, *Adv. Water Resour.*, *34*(8).

Transport in the Polymer Electrolyte Membrane

Weber-Newman model[1]:

$$\frac{\partial \xi}{\partial t} + \nabla \cdot \Psi = 0$$

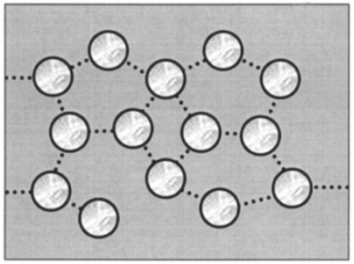

Vapor equilibrated

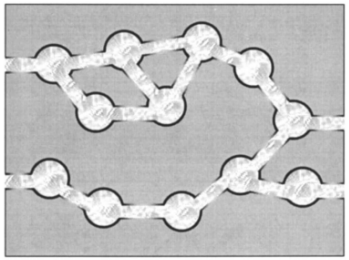

Liquid equilibrated

- **H^+:**

$$\Psi = S\left(-\sigma\nabla\Phi - \frac{\sigma n_{drag,l}}{F}\nabla\mu_{H_2O}\right) + (1-S)\left(-\sigma\nabla\Phi - \frac{\sigma n_{drag,v}}{F}\nabla\mu_{H_2O}\right)$$

- **H_2O:**

$$\Psi = S\left(-\frac{\sigma n_{drag,l}}{F}\nabla\Phi - \left(\alpha_l + \frac{\sigma n_{drag,l}^2}{F^2}\right)\nabla\mu_{H_2O}\right) + (1-S)\left(-\frac{\sigma n_{drag,v}}{F}\nabla\Phi - \left(\alpha_v + \frac{\sigma n_{drag,v}^2}{F^2}\right)\nabla\mu_{H_2O}\right)$$

- **Gas species (O_2, H_2):**

$$\Psi^k = -\psi^k \nabla p^k$$

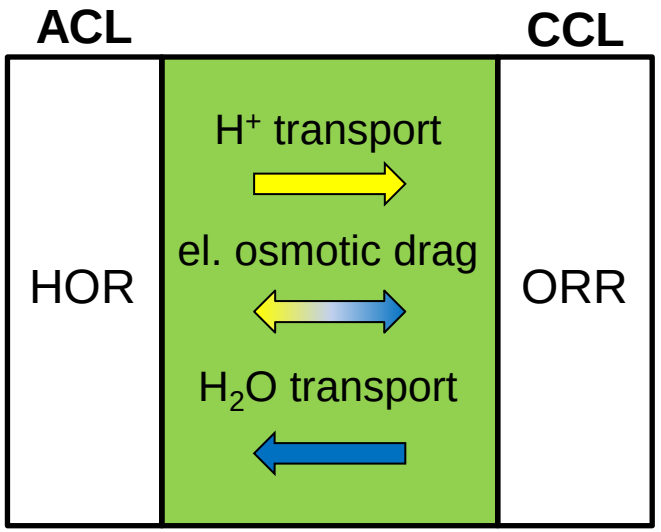

[1]: Weber, Newman, **2004**, *J. Electrochem. Soc.*, 151(2).

Electronic and Ionic Charge Balance in the Electrodes

- Electron transport in the BPPs, GDLs, MPLs, CL:

$$-\frac{\partial C_{DL}\left(\Phi_{elde}-\Phi_{elyte}\right)}{\partial t}+\nabla\cdot\left(\sigma_{eff}^{e^-}\nabla\Phi_{elde}\right)-q^{e^-}=0$$

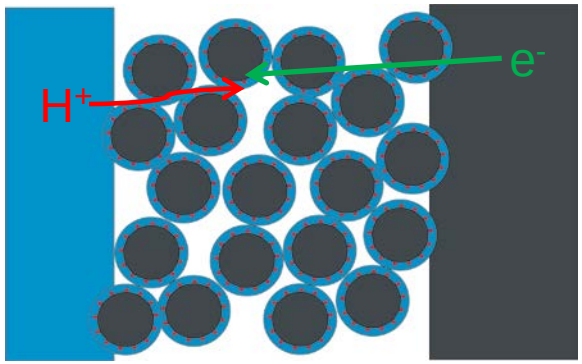

- Proton transport in the CLs:

$$-\frac{\partial C_{DL}\left(\Phi_{elde}-\Phi_{elyte}\right)}{\partial t}+\nabla\cdot\left(-\sigma_{eff}^{H^+}\nabla\Phi_{elyte}\right)-q^{H^+}=0$$

- Proton transport strongly depends on RH [1,2]

$$\sigma_{eff}^{\kappa}=\sigma^{\kappa}\left(a_{H2O}\right)$$

[1]: D. K. Paul et al., JES, 161 (**2014)** F1395.
[2]: B. P. Setzler, F. Fuller JES, 162 (**2015)** F519.

Ionomer film model

- Model for ORR reaction rate taking into account
  - Oxygen transport through ionomer film
  - Resistances at gas/ionomer and ionomer/Pt interfaces[1]

- Analytical solutions are possible for $r_{BV} \propto c_{O2}$ and $r_{BV} \propto \sqrt{c_{O2}}$

- Reaction rate for $r_{BV} \propto \sqrt{c_{O2}}$:

$$r = \frac{\sqrt{4A_{eff} n^2 F^2 c_{O2} + R^2 k^2} - Rk}{2A_{eff} nF} k$$

$$k = ECSA\ i_o c_{ref}^{-0.5} \left[\exp\left(\frac{\alpha nF\eta}{RT} \right) - \exp\left(\frac{(1-\alpha) nF\eta}{RT} \right) \right]$$

$$R = \frac{\delta_{ion}}{D_{O2,ion}} + R_{\text{int}}\left(a_{H2O}\right)$$

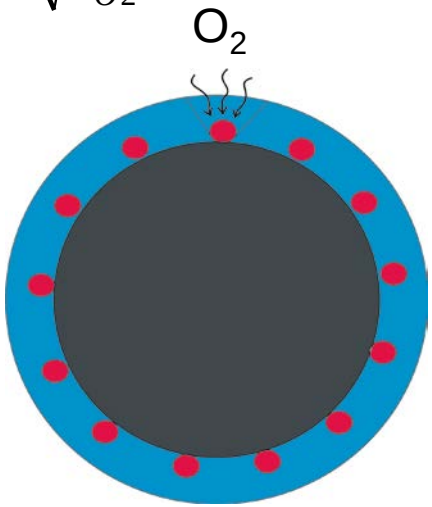

[1]: Hao et al., JES, 162 (**2015)** F854.

Numerical Treatment of Phase Transitions

NCP-equations for phase transitions[1]

- If a phase is not present:

$$\forall \alpha : S_\alpha = 0 \rightarrow \sum_{\kappa=1}^{N} x_\alpha^\kappa \leq 1 \quad (1)$$

- If a phase is present

$$\forall \alpha : \sum_{\kappa=1}^{N} x_\alpha^\kappa = 1 \rightarrow S_\alpha \geq 0 \quad (2)$$

→ $$\forall \alpha : S_\alpha \left(1 - \sum_{\kappa=1}^{N} x_\alpha^\kappa \right) = 0 \quad (3)$$

- Equations 1-3 constitute a non-linear complementarity problem
- Solution is a non-linear complementarity function:

$$\Phi(a,b) = 0$$

$$a \geq 0 \wedge b \geq 0 \wedge a \cdot b = 0$$

$$\Phi(a,b) = \min\left\{ S_\alpha, 1 - \sum_{\kappa=1}^{N} x_\alpha^\kappa \right\}$$

[1]: Lauser et al., **2011**, *Adv. Water Resour.*, *34*(8).

Model Coupling and Schroeder's Paradox

Numerical Coupling:
- Dirichlet-Neumann

Physical Coupling:
- Macroscopic Approach**:**
- Local thermodynamic equilibrium

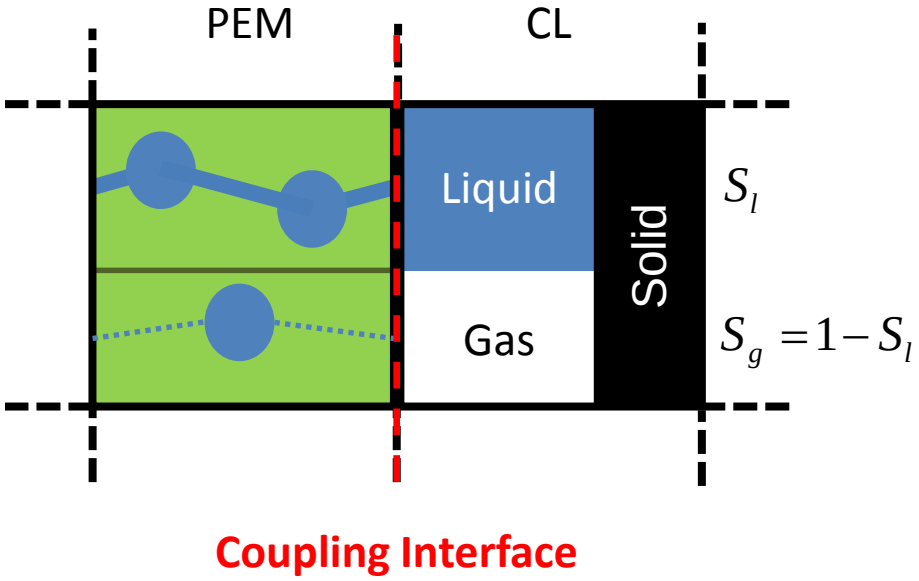

$$\lambda_l \approx 22$$

$$\lambda_g = f\left(a_{H_2O}\right)$$

$$\lambda_{PEM} = S_g \lambda_g + S_l \lambda_l$$